Heliyon 10 (2024) e27235

Contents lists available at ScienceDirect

Heliyon

journal homepage: www.cell.com/heliyon

Research article

Magnetic Fe_3O_4 /Al_2O_3 /MnO_2 ternary nanocomposite: Synthesis and characterization for phosphorus desorption from acidic soils using dialysis membrane tube

Hirpo Hinsene, Abi M.Taddesse, Endale Teju *, Yibrehu Bogale

Department of Chemistry, College of Natural and Computational Sciences, Haramaya University, P.O. Box, 138, Dire Dawa, Ethiopia

ARTICLE INFO

Keywords:
Acidic soil
Desorption
Dialysis membrane tube
Kinetics
Magnetic nanocomposite
Phosphorus

ABSTRACT

Monitoring phosphorus fertilization is crucial for controlling the concentration of biologically available soil P. Over the years, several methodologies have been used, including successive cropping in a greenhouse or field, as well as extractions employing P sink procedures. The latter procedures are ideal laboratory experiments to show the soil's ability to supply P and to explore the P-residual release kinetics. Following these methodologies, long-term P desorption studies have been developed using dialysis membrane tubes filled with nanomaterial solutions. In this study, a magnetic nanocomposite (Fe_3O_4/Al_2O_3/MnO_2) was synthesized and characterized utilizing cutting-edge instruments such as XRD, FTIR, FAAS, BET, SEM, and EDX. The resulting material had a crystalline size and surface area of 22.75 nm and 203.69 m^2/g, respectively, and was employed for long-term P-desorption and kinetics experiments while filled in dialysis membrane tubes. The P-desorption experiment was conducted on four separate acidic soil samples that were cultured for 122 days with four different P concentrations. The findings demonstrated a direct relationship between P-desorbed and P-treatment, as well as with desorption time. The minimum desorption was obtained from the control of Boji Dirmaji soil P0 (1.16–9.36) and the highest desorption from Nedjo soil with P3 (5.23–30.35 mg/kg) treatment over 1–28 days. The rate of P release from soil to solution or diffusion through the membrane was determined by pseudo-first-order kinetics with a rate constant (0.021–0.028 hr^{-1}). This method has the potential to measure fixed-P availability by mimicking it as a plant would, with high P-desorption efficiency and quick P-release capacity.

1. Introduction

Food is one of the most basic essentials for mankind to sustain life, and it is essential for all forms of life on this planet. For the vast majority of the world's population, food security is directly dependent on agriculture, which is in turn dependent on the many agro-supplements, including phosphate fertilizer, required to boost food productivity. The amount of phosphorus assimilated by plants from a field during the application of phosphorus-containing fertilizers is varied and is believed to be in the range of 3–33% of the applied phosphate fertilizer [1,2]. This is due to the high possibility of P being fixed into insoluble precipitates and sorbed in acidic soils as a result of reactivity with compounds containing Fe and Al, as well as with other colloid forms in the soil [3]. As a result of this fixation,

* Corresponding author.
E-mail address: endale.teju@haramaya.edu.et (E. Teju).

https://doi.org/10.1016/j.heliyon.2024.e27235
Received 24 May 2023; Received in revised form 17 February 2024; Accepted 26 February 2024
Available online 28 February 2024

phosphorus (P) in soil may become unavailable to plants, resulting in decreased crop output [4]. In this instance, phosphate fertilization monitoring is critical for managing the concentration of biologically accessible soil-P. Various approaches for estimating the presence of P-residual in soils for plants have been employed over the years. Experiments involving successive cropping in a greenhouse or field were used among these methods by monitoring P assimilation until deficiency occurs or by assessing the reaction of P provided to the soil [5]. However, this procedure is time-consuming and costly.

In response to these problems, soil extractions using P sink procedures, like anion exchange resins [6] and iron oxide-impregnated paper strips [5] have been developed for the estimation of fixed P. In contrast to the common soil-P testing approaches, those P sink procedures could be assumed to be non-destructive since there is no reaction between them and the soil and possess a nominal influence on the various physicochemical properties of the soil which have an impact on the P-releasing tendency. Additionally, the use of those P sink procedures controls the solution P not to increase to levels that can prohibit additional P release. As a result of this, it will be possible to undertake a series of extractions from a given soil. Hence, successive extraction of P from soils using these procedures becomes a suitable laboratory test to depict the capability in supplying P by the soil and to explore the P-residual release kinetics. Following these approaches, methods involving dialysis membrane tubes which are filled with solutions hydrous ferric oxide (DMT-HFO) have been developed [7–10].

These methods are more convenient than the P sink methods because the dialysis membrane tubes possess crucial properties like mechanical stability and can maintain low P activity for a longer period of time in the solution and simplify the estimation for the release of P over long periods of time in a more natural setting than the common soil tests [7,9,11–14]. Thus, integrating the dialysis membrane method with nanomaterials attracted a great intention towards the advancement of these methods for long-term P desorption study. In our recent study, we used dialysis membrane tubes that are filled with an aqueous solution of hydrous Fe–Al–Zr oxide composite for a phosphate desorption study [11].

To the best of our knowledge, there is no report on the use of $Fe_3O_4/Al_2O_3/MnO_2$ nanocomposite filled in a dialysis membrane tube to simulate and study the rate of P-desorption by plants from acidic soil. In view of the above points, in this particular report, we propose the use of the above-mentioned ternary nanocomposite filled in a dialysis membrane tube to study long-term P desorption and evaluate the time frame by which the fixed P in soil could be available for the plant. Therefore, in this study, a new method employing dialysis membrane tubes filled with magnetic ternary mixed oxide nanocomposite ($Fe_3O_4/Al_2O_3/MnO_2$) was developed to study the tendency of long-term P desorption from acidic soils which is of paramount advantage for fertilizer recommendation for a given agricultural activity. The P-releasing rate from soil to solution or diffusion through the membrane was studied. The as-synthesized nanocomposite was characterized using different analytical methods and instruments. Similarly, the various physico-chemical parameters affecting the P-desorption process were also investigated.

2. Materials and methods

2.1. Description of the study area

Acidic soil samples used in the various experimental undertakings of the present study were obtained from selected areas of West Wollega Zone, Oromia Region, Ethiopia located at about 477–575 km west of Addis Ababa, the capital city, with a geographical location of 09° 51′ 28'' - 09° 25′ 33″ N latitude and 35°36' 28'' - 35° 02′ 13″ E longitude with an elevation between 1845 and 1930 m. The area has an altitude (1300–1800 masl), annual rainfall (1000–2400 $mmyr^{-}1$), and temperature (12.5–29 °C) [15]. The soil samples were collected from four districts, Boji Dirmaji (BD), Kiltu Kara (KK), Mene Sibu (MS), and Nedjo (NE) which are acidic in nature [16]. The soil was randomly collected from farmers' crop fields.

2.2. Soil sample collection

Stainless steel augur was used to collect surface soil samples (0–20 cm depth), required for the various experiments, randomly from each sampling site based on USDA methods [17]. The collected samples were carefully mixed to get a composite sample and a total of four composite soil samples were collected and packed in plastic bags, labeled, and transported to the department's research laboratory for the intended analysis. Then the soil samples were air dried at room temperature for 7 days, ground, to pass through a 2 mm mesh size sieve for physicochemical parameter analyses. For the desorption study, 5 kg of the collected soil samples were prepared in a plastic pot and spiked with known concentrations of P in the form of KH_2PO_4 and incubated in a greenhouse for about three months and twenty-two days at field capacity [14].

2.3. Materials and chemicals

2.3.1. Materials

The instruments used in this study were; pH meter (MP 220 JENWAY, Japan) used for determination of pH, X-ray diffractometer (XRD) (BRUKER D8 Advanced XRD, Japan), which was used for the determination of size and phase of the as-synthesized powder sample, Fourier transform infrared spectroscopy (FTIR) (spectrum 65 FTIR PerkinElmer) used for functional group identification of the as-synthesized adsorbent, Uv–Visible spectrophotometry (Uv professional, Galanakamp, UK) used to analyze the concentrations of P, BET (JW-04, Beijing), SEM (HITACHI S-4160, UK), EDX (VEGA\\-TESCAN, base director, German), Deionizer (B114, Oxford, UK), and Orbital shaker (S01 Stuart, UK), Flame atomic absorption spectrophotometer ((Model 210/211 VGP, UK) and Micro Kjeldahl distillation unit and Kjaldahl digestion stand (for total nitrogen determination), Analytical balance (Denver Instrument XE 50A),

Conductivity meter (model CO155), Centrifuge (Centurion scientific, UK), Refrigerator and Hydrometer, which used for texture determination.

2.3.2. Chemicals and reagents

The various chemicals and reagents used in the different experimental undertakings of the present study were of analytical grade and used as received. Some of the chemicals and reagents used were; Aluminum nitrate nonahydrate ($Al(NO_3)_3.9H_2O$) (95%–98% Merck Germany), Ferrous chloride tetrahydrate ($FeCl_2.4H_2O$), Ferric chloride hexahydrate ($FeCl_3.6H_2O$) (LOBAL chemie, India) and Manganese (IV) oxide (MnO_2) (BDH Chemicals Ltd, England), which were used for the synthesis of the sorbent. Potassium dihydrogen phosphate (KH_2PO_4) (99–101% High-tech healthcare, India), Potassium chloride (KCl, 99.0% loba, India), Ammonium fluoride (NH_4F, 99.5%, Switzerland), Hydrogen peroxide (H_2O_2, 30% Central Drug House LTD, New Delhi, India), Sulfuric acid (H_2SO_4, 98%, laboratory reagent, loba, India), Nitric acid (HNO_3) (69% LR, Breck land Scientific Supplies, U. K), Potassium antimony tartarate ($KSbC_4H_4O_7$ (98.5% BDH Chemicals Ltd, England) to know the total, available and P desorbed by the adsorbent, Calcium chloride ($CaCl_2$) (High-tech Healthcare, India). Ammonium molybdate tetra hydrate ($(NH_4)_6Mo_7O_{24}.4H_2O$) (81–83 % Riedel DeHaen AG), Ascorbic acid, ($C_6H_8O_6$) (99% Blux laboratory reagents) were used for the determination of phosphate colorimetrically. Hydrochloric acid (HCl), 36–37%, and Sodium hydroxide (NaOH), 97.5% from BDH Chemicals Ltd, England) were used for adjusting pH during the nanocomposite synthesis.

2.4. Experimental procedures

2.4.1. Standard solution preparation

A stock standard solution of P (1000 mg/L) was prepared by dissolving 4.39 g of KH_2PO_4 in 1 L of deionized water. The intermediate standard solution (10 mg/L) was prepared by suitable dilution of the stock solution and the working standard solutions were obtained by serial dilution of the intermediate standard solution and used for P analysis.

2.4.2. Synthesis of the nanomaterials

2.4.2.1. Synthesis of Fe_3O_4. Synthesis of magnetic Fe_3O_4 nanoparticles was done by co-precipitation of ferric and ferrous salts under N_2 gas [18]. The mole ratio of Fe^{+2}/Fe^{+3} (0.5) was used to prepare homogeneous magnetic nanoparticles with uniform size [19]. In the first step stoichiometrically calculated (8.63 and 3.17 g) of $FeCl_3$.$6H_2O$ and $FeCl_2$.$4H_2O$, respectively, were accurately measured and dissolved into 100 mL of 0.3 M HCl [20]. The resulting solution was then added dropwise from the separatory funnel into 120 mL of 3 M NaOH solution for 2 h, with vigorous stirring at 80 °C under N_2 atmosphere. At this time, the pH of the mixture was kept at 12.0 by using 0.1, 0.01 and 0.001 M NaOH or HCl solutions. The suspension was left undisturbed for 4 h and the settled phase was separated and washed with deionized water several times. This action was repeated until the time when the addition of $AgNO_3$ solution to the filtrate show no formation of white precipitate. Finally, a suspension of Fe_3O_4 (ferrofluid) was obtained [21,22].

2.4.2.2. Synthesis of $Fe_3O_4/Al_2O_3/MnO_2$ nanocomposite. The $Fe_3O_4/Al_2O_3/MnO_2$ ternary nanocomposite was prepared by the co-precipitation method [18]. As a synthesis protocol, three different compositions of $Fe_3O_4/Al_2O_3/MnO_2$ with Fe:Al:Mn percent ratios (%) (90, 5, 5), (80, 15, 5) and (70, 15, 15) or molar ratios of 18:1:1, 16:3:1 and 14:3:3, respectively, were prepared. This was done by adding 100 mL of $Al(NO_3)_3.9H_2O$ and MnO_2, which were obtained by dissolving stoichiometric amounts (2.25 and 0.09 g) of each, respectively, in 100 mL of deionized water separately, into the obtained Fe_3O_4 suspension and ultrasonicated for 10 min before use. Next to this, the pH of the mixture was adjusted to 8.0 using 0.1, 0.01 and 0.001 M NaOH or HCl. This step was followed by magnetically stirring the mixture under N_2 for 1.5 h at 70 °C. Finally, the black magnetic fluid was made to settle by holding a permanent magnet under the beaker. The product obtained as such was then washed with deionized water repeatedly to remove impurities such as Cl^-, NO_3^- and excess OH^-ions and finally dried at 60 °C for 24 h to get the desired products [22].

2.4.3. Characterization of as-synthesized nanocomposite

X-ray diffraction (XRD) patterns were recorded by a diffractometer at 0.02°/sec scan rate using Cu-kα1 radiation (1.5406 A^0, 45 kV, 40 mA) and used to determine sizes of the primary crystallite (Ds) of the nanocomposite It is also used to identify the phase of the as-synthesized nanocomposite. Similarly, Fourier transform-infrared (FTIR) spectra was recorded over the range of 400–4000 cm^{-1} using a Spectrometer for functional group identification of the as-synthesized nanocomposite. Scanning Electron Microscopy (SEM) and Energy Dispersive X-ray Analysis (EDX), were used to determine the morphology and compositional distribution of the nanocomposite, respectively in which the nanocomposite was coated on conductive carbon tape attached on aluminum stub. The percentages of iron as iron oxide and manganese as manganese oxide in all the as-synthesized powders were investigated using a flame atomic absorption spectrometer (FAAS). On the other hand, Brunauer Emmett-Teller (BET) was used to determine the surface area of the prepared nanocomposite.

2.5. Physicochemical properties of soil samples

The soil samples were air-dried, ground and allowed to pass through a 2 mm mesh-size sieve and homogenized and the selected soil physicochemical were performed. The pH in water and KCl of the soil samples were measured by dispersing 1:2.5 soil to water ratio

[9]. The electrical conductivity was determined using 1:5 ratios of soil-to-water [23]. The soil texture was evaluated by the hydrometer method [24] and soil texture class was determined based on the USDA [25]. Bulk density was determined gravimetrically after oven drying the soil sample for 24 h at 105 °C [26]. Soil organic carbon was analyzed by oxidation with 1 N of $K_2Cr_2O_7$ [13,27]. Soil organic matter was obtained multiplying organic carbon by 1.724 [27,28]. Exchangeable acidity was determined by saturating (10 g) of the soil samples with 100 mL of 1 M standard potassium chloride solution [13]. Total nitrogen was determined by the Kjeldahl method using a micro Kjeldahl distillation unit and Kjeldahl digestion stand [14].

Cation exchange capacity (CEC) was measured using 1 M NH_4OAc and the available phosphorus in the soil sample was determined based on the Bray II method [29]. Total soil P (TP) was determined on sub-samples of 0.5 g soil with the addition of 5 mL concentrated H_2SO_4 and heating to 360 °C on a digestion block with subsequent stepwise (0.5 mL) additions of H_2O_2 until the solution becomes clear [9]. The phosphate bounded Fe and Mn in the soil samples were investigated by dithionite–citrate and acid ammonium oxalate methods [30].

2.6. Incubation study

In the present study, greenhouse was used for incubation experiments. Four treatments of P as KH_2PO_4 with concentrations of 0 (P0), 50 (P1), 100 (P2) and 150 (P3) mg/kg were added to soil samples of 5 kg separately and incubated at 25 °C for 112 days. Then the incubated soil was used to study long term desorption of P and kinetic studies using DMT-HFAMO [14].

2.7. Long-term desorption study

The long-term P-desorption experiment in this particular study was performed using dialysis membrane tubes (Visking, size $3^{20/32}$ inches, with a pore size of 2.5–5.0 nm, membrane thickness 3 μm, MWCO 12000 kDa) [9,10,12,13] filled with the nanocomposite prepared in this study. In this particular experiment, we followed the following procedure; the aforementioned tube was cut into 0.15 m strips and 20 mL of 0.1 g of the HFAMO nanocomposite was added to each strip with vigorous shaking. Following this, the HFAMO-filled DMT strips were immersed separately in 250 mL polyethylene bottles which contained 1 g of the soil sample, 80 mL of 2 mM $CaCl_2$ and 0.3 mM KCl solution. The P-desorption experiments were performed in three replication and the polyethylene bottles were horizontally shaken for 28 days on an end-over-end shaker at 120 oscillations per minute (opm) at room temperature (25 °C) [11].

During this experiment, each DMT-HFAMO was replaced in an interval of seven days (1, 7, 14, 21 and 28) with new DMT-HFAMO by removing any attached soil particle on the dialysis membrane tube carefully with a glass rod. Then the suspension was dissolved using 1 mL of concentrated H_2SO_4 and the concentration of P in the solution was determined colorimetrically using the molybdate blue method that makes use of ascorbic acid as a reducing agent [11]. Each reagent was mixed and prepared by taking 50 mL of ammonium molybdate solution, 5 mL of potassium antimony tartrate solution and 0.553 g of ascorbic acid in 100 mL volumetric flasks. Then, 2 mL of the mixed reagent was mixed with 2 mL of the sample filtrate in a 25 mL conical flask and left for 30–40 min till a blue color develop. The intensity of the blue color correlates to the concentration of phosphate. Finally, a Uv–Visible spectrophotometer was used to analyze the concentration of P in the soil samples at a wavelength of 882 nm. All determinations were conducted in triplicate, and the results are reported as mean ± standard deviation.

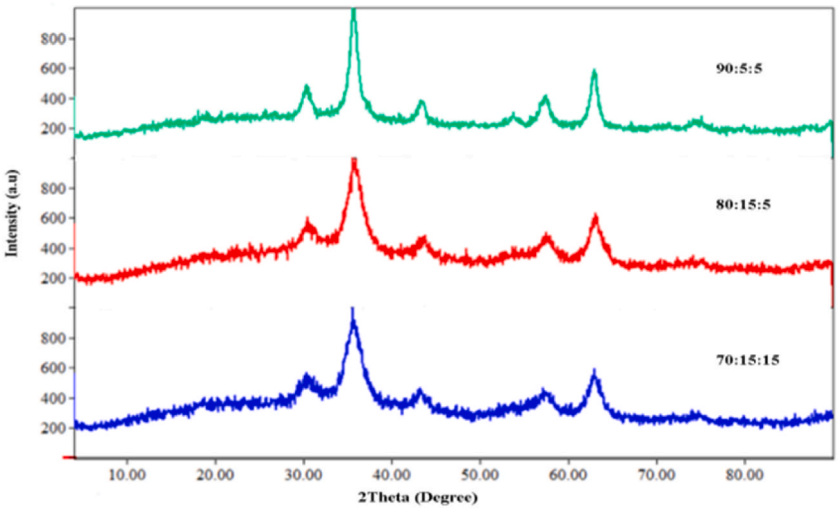

Fig. 1. XRD pattern of as-synthesized ternary mixed oxide nanocomposites.

2.8. Data analysis

In the present study, a one-way analysis of variance (ANOVA) using SAS version 9.0 was employed to test significant differences among treatments and a correlation analysis was conducted to test the relationship between cumulative desorbed P (CD28P) and the corresponding selected soil physicochemical parameter by SPSS. The FTIR spectra were plotted using Origin 70 and MS excel was used to draw calibration curve. The Match 2 software was used to determine the size and phase identification.

3. Results and discussion

3.1. Characterization of as-synthesized adsorbent

The X-ray diffraction pattern shows very weak intensities on a broad background suggesting a slightly amorphous nature of the synthesized nanocomposite (Fig. 1). The average crystallite size was also determined from Scherer equation as shown in Table 1.

The peaks observed on the three nanocomposites appeared to be almost similar. The presence of peaks at 2θ values of (30.70, 35.80, 43.51, 54.04, 57.37, 62.90 and 74.76)^{o} [JCPDS: 96-900-5815] for NC_1, (30.49, 35.84, 43.62, 57.48, 63.31 and 74.86)^{o} [JCPDS: 96-900-5842] for NC_2 and (30.80, 35.70, 43.31, 57.06, 62.90 and 74.53)^{o}[JCPDS: 96-900-2023] for NC_3 could be assigned to a face-centered cubic spinel structure of pure magnetite (Fe_3O_4) [31]. However, no specific peaks were observed that can be attributed to alumina (Al_2O_3) and manganese (MnO_2) implying that both might exist in amorphous forms at the temperature of synthesis and due to the low percentage of MnO_2 [32]. In fact, crystallized alumina such as α-Al_2O_3 and β-Al_2O_3 might present under thermal treatment at 800 °C and 1000 °C, respectively [33]. In other cases, our findings indicated that the particle sizes of the nanocomposites increased with a decrease in the percentage of alumina in the samples and similar trends were reported [34]. However, increasing alumina oxide could delay the crystallization of iron oxides and shrink the size of the crystallites. The concomitant increase in manganese oxide could have a counter effect which might have led to increasing crystal size as reported in the literature [35] and this is due to the formation of core-shell structured nanoparticles or composite (magnetite as core and manganese oxide as a shell) [36]. Besides, the presence of a large amount of manganese dioxide powder delays the uniformity of the nanocomposite [37]. Generally, the XRD result confirmed the synthesis of the ternary nanocomposite in a good crystalline range of 10–50 nm (Table 1) [38].

The three nanocomposites synthesized in the present study were investigated for their specific surface areas using both single-point and multi-point BET analytical methods. Based on the results obtained, the comparative specific surface areas were found in the order of NC_2 (80:15:5) > NC_3 (70:15:15) > NC_1 (90:5:5) (Table 1). The nanocomposite with the smallest size was found to show the highest surface area in line with the reports in the literature [33,39]. This implies that the adsorbent material exhibits more active sites for the adsorption process. This is mainly because adsorption is a surface phenomenon and the surface area is directly proportional to the adsorptive performance of the adsorbent material. Hence, NC_2 with the ratio of (80% Fe, 15% Al and 5% Mn), resulted in relatively the highest specific surface area and was selected for further analysis and used for the desorption study. Nanomaterials exhibiting high specific surface area, high surface activity, and high surface energy, appear to show higher capacity in the preparation of high-performance adsorbents and materials [40,41].

The infrared spectroscopic study of the selected Fe–Al–Mn nanocomposite was undertaken and the results obtained are presented in Fig. 2. In the spectrum, it can be clearly observed that the major absorption peaks are located at 3414, 1628, 1384, 587 and 443.6 cm^{-1}. Accordingly, the absorption peak at 3414 cm^{-1} represents O–H stretching vibration of the adsorbed water molecules [34,42]. The absorption peak at 1628 corresponds to the bending vibrations of the H–*O*–H group and may be assigned to the presence of physisorbed water on the surface of oxides [43] and the peak at 1384 cm^{-1} corresponds to the Al–O stretching [44]. The peaks at 587 cm^{-1} and 443.6 cm^{-1} can be attributed to the symmetrical stretching vibrations of the mixed metal oxides M − O and M-*M*-O [45] or Fe–O (Fe_3O_4) bond presence in the nanocomposite and an example of some interactions among Fe(III), Al(III) and Mn(IV) though oxygen or hydroxide bridge [46].

Elemental composition of the selected nanocomposite (NC_2 (80:15:5)) was analyzed with flame atomic absorption spectrometer (FAAS) by using air-acetylene gas as an oxidant for Fe and Mn. The results corresponding to the percentages of iron and manganese oxides are obtained at wavelengths of 248.3 and 279.5 nm, respectively. The results indicated (Table 2) that the percentage compositions of the two metals (Fe and Mn) in the selected nanocomposite (NC_2) were found to be nearly similar to the theoretical composition of the metals. However, the actual values are lower than the theoretical values. This difference in the percentage compositions could be related to insufficient dissolution, vaporization and lack of atomization [22,35]. Aluminum was not determined due to lack of nitrous oxide gas (oxidant).

The SEM-EDX analysis revealed the morphology and also elemental composition of the nanocomposite. From the SEM image of the nanocomposites of various ratios, all the samples exhibited irregular particles of various sizes with no distinct morphology (Fig. 3 A – C). EDX analysis of the micrographs showed the presence of all three metals (Al, Fe, and Mn) and the weight of each metal in the

Table 1
Surface area (m^2/g) and particle sizes (nm) of the nanocomposite with different compositions.

Sample Code	% Composition of Fe–Al–Mn	2θ (degree)	β (rad)	Cosθ	Ds (nm)	Surface area (m^2/g)
NC_1	90:5:5	35.80	0.00550	0.9516	26.51	114.38 ± 0.69
NC_2	80:15:5	35.84	0.00641	0.9513	22.75	203.69 ± 1.34
NC_3	70:15:15	35.70	0.00579	0.9519	23.93	193.95 ± 1.29

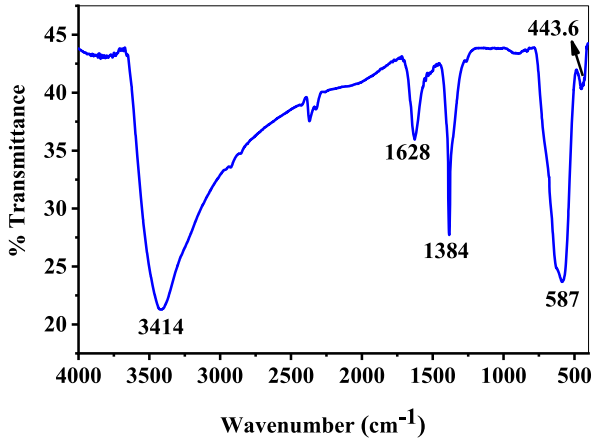

Fig. 2. FTIR spectrum of the selected nanocomposite.

Table 2
Actual and theoretical yield of the selected nanocomposite.

Elements	Theoretical yield (%)	Actual yield (%)
Fe	80	78.82
Al	15	ND[a]
Mn	5	4.20

[a] ND = Not determined.

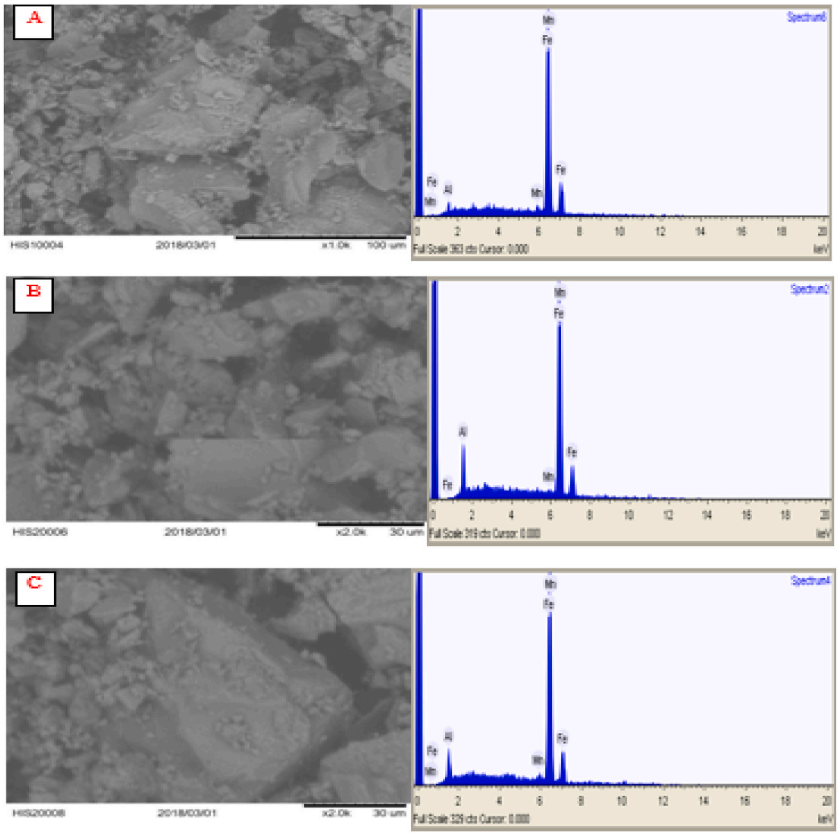

Fig. 3. SEM-EDX of Fe–Al–Mn ternary mixed oxide nanocomposites (A = NC_1, B═NC_2, C═NC_3).

nanocomposites was confirmed in different ranges. A relatively wider range of composition was registered (Table 3) for each element revealing the heterogeneity of the composites [32]. The observed slight variation of the Fe–Al–Mn metals percent weight ratio distribution might be due to the dispersion technique employed in the co-precipitation method [47].

3.2. Physicochemical properties of the soil samples

The physicochemical properties of the soil samples are presented in Table 4. Based on the results obtained, the soil pH, both pH in H_2O and pH in KCl of the soils were analyzed and found to be within 4.35–5.06 and 3.54–3.79, respectively. Even though the pH variation is not so large, there was a significant difference between each soil sample ($\alpha = 0.05$). According to acidity classification, soil collected from Boji Dirmaji (pH = 4.35) can be categorized as very strongly acidic and soil collected from Nedjo (pH = 5.06) could be categorized as strongly acidic [16]. According to related reports [48], decreasing of the soil pH in western and southern Ethiopia was due to intensive rainfalls that can leach soluble nutrients such as calcium and magnesium and with subsequent replacement by Al^{3+} and H^+ ions. A pH value of less than 5.5 is considered to cause problems for most microbial activities and hence results in a direct influence on the availability of nutrients for plants.

The relative percentages of soil texture of the studied district soil samples were found as Sand (58, 66, 66 and 71), Silt (15, 7, 12 and 8) and Clay (27, 27, 21 and 22) for Boji Dirmaji (BD), Kiltu Kara (KK), Mene Sibu (MS) and Nedjo (NE) sampling locations, respectively, and the soils textural class is sandy clay loam for all soils [25]. Crops could grow well in such soil areas and it has a potentially well-balanced capacity to retain water, form a stable structure and provide adequate aeration [49]. The Bulk density value was significantly different for each soil sample ($\alpha = 0.05$); however, numerically the highest mean (1.33 g/cm^3) value of bulk density was recorded for KK and the lowest average value (1.14 g/cm^3) for the BD soil. Generally, all the soil samples had low bulk density except KK which has a moderate value (Table 4). A bulk density value of about 1.33 g/cm^3 was generally considered optimum for plant growth [50].

All district soil samples have electrical conductivity (EC) values ranging from 0.019 to 0.080 dS/m and lie within the lower limit of saline soil [23]. The organic carbon (OC) was also found to be higher in NE and lower in MS. all the studied soils fall in the low range despite the various amount extracted from the soils. According to reports, OC is the main source of available P, but in most soil of Ethiopia, the availability of P declines by the impacts of fixation, abundant crop harvest and erosion [51]. The significance difference analysis showed a significant difference ($\alpha = 0.05$) among the studied soils for both EC and OC. In addition, the organic matter (OM) of MS soil was found to be very low while the others have low and ordered as MS < KK < BD < NE. Organic matter usually has a significant effect on soil physicochemical properties, plant nutrition, soil fertility, and biological activity in a given soil. Even though a significant difference was observed among the soil samples ($\alpha = 0.05$), the OM of the soil is deficient for plant growth and this may also come from loss of OC.

Furthermore, total nitrogen (TN) compositions of the soil samples were also found to be in the ranges of 0.03–0.22%. Among studied soil samples, total nitrogen was very low for NE (0.03%) and medium in other soils. There was a significant difference ($\alpha = 0.05$) among the soils. Additionally, cation exchange capacity (CEC) was rated as moderate for both BD and KK (24.37 and 19.33 meq/100 g), respectively, and higher for MS and NE with a significant difference among each soil ($\alpha = 0.05$).

Exchangeable acidity (EA) is another key parameter related to the acidity of soil, which is the sum total of reactive hydrogen ions and exchangeable aluminum. In the present study, the result indicated that the soils have a highly acidic nature having >2 meq/100 g except for NE (1.691 meq/100 g). The high soil EA in the BD soil might be in connection with the occurrence of lower soil pH [13]. Extractable aluminum is highly consistent with pH of the soil and when extractable aluminum is > 2 meq/100 g, sensitive plants will be affected. The content of the H^+ in the soil is pronounced at pH values below 4 while excess content of Al^{3+} was observed at pH below 5.5 (Table 4).

The available P (P_{av}) of the study area was in general found to be low. In addition, differences in available P content in soil are also related with the high soil weathering or soil disturbance, and the degree of P fixation by Fe, Al and Ca [15,52]. Low P_{av} status could also be as a result of low pH and high exchangeable acidity [48]. The total P (P_T) concentration showed a similar trend like the available P concentration and ranged from 330 to 550 mg/kg. The total P concentration of Ethiopian soil reported by similar studies ranged from 553 to 976 mg/kg [15].

In examining phosphate bounded Fe and Mn, the percentages of Fe and Mn extracted by dithionite citrate bicarbonate and acid ammonium oxalate methods, the amount of Fe_{ox}, Mn_{ox}, Fe_d and Mn_d extracted were found to be significant ($\alpha = 0.05$) among the studied soil samples. Even though the dithionite citrate bicarbonate extracted elements are higher, the ammonium oxalate extractable Fe and Mn are also high evidencing the involvement of poorly crystalline and amorphous forms of Fe and Al in the soil. These structural forms have an extensive surface area to sorb P. The percentage of Fe extracted by the dithionite citrate bicarbonate method was higher than the percentage of Fe extracted by the acid ammonium oxalate method and this agrees with similar studies [13,53].

Table 3
EDX results of aluminum, iron and manganese elements in the nanocomposite.

Elements	Weight range (%)	Weight average (%)
Fe	84.8–98.5	95.1 ± 4.05
Al	0.6–11.3	3.4 ± 3.38
Mn	0.8–2.6	1.6 ± 0.56

Table 4
Selected physicochemical characteristics of the acidic soil samples studied (n = 3).

Parameters		Soil Samples				LSD (5%)
		BD	KK	MS	NE	
pH (1:2.5)	H_2O	4.35 ± 0.024^{d}	4.62 ± 0.003^{c}	4.80 ± 0.003^{b}	5.06 ± 0.011^{a}	0.03
	KCl	3.54 ± 0.010^{d}	3.61 ± 0.006^{c}	3.70 ± 0.001^{b}	3.79 ± 0.006^{a}	0.01
EC (dS/m)		0.019 ± 0.101^{d}	0.08 ± 0.050^{a}	0.022 ± 0.401^{c}	0.033 ± 0.134^{b}	0.001
Ex A.	meq/100g	4.16 ± 0.006^{a}	3.48 ± 0.028^{b}	2.73 ± 0.002^{c}	1.69 ± 0.009^{d}	0.03
Ex Al.		3.37 ± 0.030^{a}	2.61 ± 0.005^{b}	2.62 ± 0.005^{b}	1.18 ± 0.002^{c}	0.03
Ex H^{+}.		0.79 ± 0.029^{b}	0.87 ± 0.002^{a}	0.11 ± 0.031^{d}	0.51 ± 0.008^{c}	0.04
%OC		0.95 ± 0.006^{b}	0.69 ± 0.014^{c}	0.51 ± 0.009^{d}	1.05 ± 0.011^{a}	0.02
%OM		1.64 ± 0.011^{b}	1.18 ± 0.025^{c}	0.88 ± 0.015^{d}	1.80 ± 0.019^{a}	0.03
%TN		0.18 ± 0.003^{c}	0.22 ± 0.003^{a}	0.21 ± 0.004^{b}	0.03 ± 0.001^{d}	0.01
CEC	meq/100g	24.37 ± 0.651^{c}	19.33 ± 0.640^{d}	32.40 ± 0.800^{a}	26.43 ± 1.040^{b}	1.51
P_{av}	mg/kg	3.53 ± 0.017^{d}	10.11 ± 0.047^{a}	5.62 ± 0.056^{c}	9.95 ± 0.062^{b}	0.09
P_T		330 ± 0.151^{d}	390 ± 0.468^{c}	411 ± 0.695^{b}	550 ± 0.549^{a}	0.94
Fe_{ox}	g/kg	0.27 ± 0.530^{a}	0.27 ± 0.010^{a}	0.12 ± 0.150^{c}	0.15 ± 1.000^{b}	1.07
Mn_{ox}		0.069 ± 0.020^{c}	0.06 ± 0.001^{d}	0.07 ± 0.060^{b}	0.10 ± 0.050^{a}	0.84
Fe_d		0.83 ± 0.050^{b}	1.02 ± 0.040^{a}	0.30 ± 0.020^{d}	0.80 ± 0.050^{c}	0.08
Mn_d		0.10 ± 0.080^{b}	0.08 ± 0.040^{c}	0.43 ± 0.080^{a}	0.03 ± 0.050^{d}	0.12
Bd	g/cm^3	1.14 ± 0.003^{d}	1.33 ± 0.001^{a}	1.16 ± 0.003^{c}	1.26 ± 0.006^{b}	0.01
Soil Texture	% sand	58	66	66	71	
	% silt	15	7	12	8	
	% clay	27	27	22	21	
	class	Sandy clay loam	Sandy clay loam	Sandy clay loam	Sandy clay loam	

Mean values in the rows with different letters a, b, c and d are significantly different (α = 0.05).
BD = Boji Dirmaji Soil, KK = Kiltu Kara Soil, MS = Mene Sibu Soil, NE = Nedjo Soil, P_{av} = Available P, Bd = Bulky density, CEC = Cation exchange capacity, EC = Electrical conductivity, Ex.A = Exchangeable acidity, Ex.Al = Exchangeable alumni, Ex.H^{+} = Exchangeable hydrogen, OC = Organic carbon, OM = Organic matter, TN = Total nitrogen, P_T = Total phosphorus, Fe_d = Iron extracted by dithionite, Mn_d = Manganese extracted by dithionite, Fe_{ox} = Iron extracted by oxalate, Mn_{ox} = Manganese extracted by oxalate, CV = Coefficient of var-iation (%), LSD = Least significance difference (5%), n = Number of replication.

3.3. Long-term desorption study

Long-term P desorption was carried out using the DMT-HFAMO on four acidic soils namely Boji Dirmaji (BD), Kiltu Kara (KK), Mene Sibu (MS) and Nedjo (NE). All soil samples received P doses of 0, 50, 100 and 150 mg/kg and were equilibrated for three months and twenty-two days at field capacity. The amount of desorbed P by DMT-HFAMO was significantly affected (α = 0.05) by both the P treatments and extraction time (Tables 5 and 6). Among all treatments, the amount of DMT-HFAMO extractable P significantly

Table 5
Desorption of phosphorus from soil and effect of extraction time for soil samples with different treatment (n = 3).

Soil Samples	P Treatments (mg/kg)	Cumulative desorbed P (mg/kg) per days					
		1	7	14	21	28	Average P (mg/kg)
BD	0	z1.16 ± 0.01^{c}	y3.01 ± 0.09^{d}	x5.43 ± 0.18 ^{d}	w7.62 ± 0.09^{d}	v9.36 ± 0.16^{d}	5.316
	50	z3.65 ± 0.11^{b}	y8.31 ± 0.14^{c}	x13.16 ± 0.03^{c}	w18.13 ± 0.24^{c}	v22.77 ± 0.34^{c}	13.29
	100	z3.71 ± 0.06^{b}	y8.98 ± 0.44^{b}	x14.32 ± 0.79^{b}	w19.43 ± 0.92^{b}	v24.50 ± 0.78^{b}	14.19
	150	z4.70 ± 0.08^{a}	y10.41 ± 0.9^{a}	x16.09 ± 0.39^{a}	w21.24 ± 0.31^{a}	v26.86 ± 0.79^{a}	15.86
LSD (5%)		0.14	0.45	0.86	0.95	1.10	
KK	0	z1.01 ± 0.0^{d}	y3.27 ± 0.10^{c}	x5.75 ± 0.09^{d}	w7.99 ± 0.10^{d}	v9.57 ± 0.09^{d}	5.52
	50	z4.30 ± 0.09^{c}	y9.74 ± 0.41^{b}	x14.99 ± 0.26^{c}	w20.06 ± 0.03^{c}	v24.36 ± 0.22^{c}	14.69
	100	z4.57 ± 0.12^{b}	y10.12 ± 0.12^{b}	x15.84 ± 0.37^{b}	w21.18 ± 0.77^{b}	v25.84 ± 1.11^{b}	15.51
	150	z4.90 ± 0.17^{a}	y10.73 ± 0.07^{a}	x17.05 ± 0.48^{a}	w23.47 ± 0.49^{a}	v28.13 ± 0.55^{a}	16.86
LSD (5%)		0.22	0.41	0.63	0.86	1.19	
MS	0	z1.32 ± 0.02^{d}	y4.07 ± 0.09^{d}	x6.23 ± 0.10^{d}	w8.74 ± 0.09^{d}	v10.80 ± 0.16^{d}	6.23
	50	z4.15 ± 0.09^{c}	y9.56 ± 0.11^{c}	x14.52 ± 0.32^{c}	w20.02 ± 0.44^{c}	v25.36 ± 0.55^{c}	14.72
	100	z4.62 ± 0.22^{b}	y10.55 ± 0.36^{b}	x16.08 ± 0.36^{b}	w21.67 ± 0.08^{b}	v27.45 ± 0.54^{b}	16.07
	150	z5.19 ± 0.25^{a}	y11.93 ± 0.49^{a}	x18.35 ± 0.71^{a}	w24.06 ± 0.44^{a}	v30.10 ± 0.27^{a}	17.93
LSD (5%)		0.32	0.59	0.81	0.59	0.78	
NE	0	z1.43 ± 0.7^{d}	y4.02 ± 0.0^{d}	x6.39 ± 0.09^{d}	w9.01 ± 0.14^{d}	v11.29 ± 0.16^{d}	6.43
	50	z4.12 ± 0.17^{c}	y9.78 ± 0.31^{c}	x14.89 ± 0.39^{c}	w20.14 ± 0.89^{c}	v24.55 ± 0.85^{c}	14.70
	100	z4.71 ± 0.14^{b}	y10.59 ± 0.14^{b}	x16.99 ± 0.53^{b}	w22.40 ± 0.67^{b}	v27.65 ± 0.46^{b}	16.47
	150	z5.23 ± 0.22^{a}	y11.91 ± 0.16^{a}	x18.52 ± 0.36^{a}	w24.32 ± 0.24^{a}	v30.35 ± 0.51^{a}	18.07
LSD (5%)		0. 33	0.40	0.75	1.13	1.08	

BD = Boji Dirmaji Soil, KK = Kiltu Kara Soil, MS = Mene Sibu Soil, NE = Nedjo Soil. Mean.
values in rows with different letters z, y, x, w and v are significantly different (α = 0.05), while mean values in the columns with different letters a, b, c and d are significantly different (α = 0.05), Least significance difference (5%), n = number of replicate measurements.

increased as extraction time and treatment of phosphate increased (Table 5). The cumulative P desorbed was more or less comparable among the studied soil samples; NE (1.43–30.35 mg/kg), MS (1.32–30.10 mg/kg) KK (1.01–28.13) and BD (1.16–26.86 mg/kg) at all stages of extraction time (1–28 days). These results agreed with earlier reports [1,9,14]. When the cumulative desorbed P is compared with the total P (Table 4), it is very low. This may be due to the presence of high extractable Fe and Al in the studied soil that can reduce the desorption process as a result of the formation of phosphate complex in acidic soil and incubation. Additionally, the amount of desorbed P from the untreated soil during the 28 days of extraction was much higher than Bray II P (P_{av}) for soil samples collected from BD and MS whereas comparable amount with Bray-II P (P_{av}) for soil samples from NE and KK (Tables 5 and 6). This signifies that the method can extract residual P as time increases just like plants could take residual P during their growing season.

As can be seen from Table 6, when soil samples with similar treatments were compared, almost comparable amount of P was desorbed with the corresponding desorption time and no statistically significant difference was observed in most cases ($\alpha = 0.05$). In addition, the cumulative desorbed amount of P that was extracted using DMT-HFAMO within 28 days was found to be very low when compared to the total P, but it was larger when compared with the available P. This indicates that the physicochemical characteristics of the soil samples are nearly similar which influenced desorption of P in the same manner [11]. Small amounts of significant difference in some of the soil samples with the same treatments ($\alpha = 0.05$) (Table 6) might be due to differences in the nature of the soil [13,14,54].

As Fig. 4 (a – d) illustrates no desorption plateau was observed during the extraction time and this indicates desorption can continue for a longer period than 28 days or 672 h [9,54,55]. The data fitness test indicated that the values well fitted to the linear regression equations and the R^2 values indicate meaningful correlations among treatments and the desorbed P. Generally, the degree of desorption of P for a given treatments had an order of P0 < P1 < P2 < P3 for all soil samples within 28 days of desorption time and it was in agreement with the result of related work [14]. The equilibrium not achieved indicate that desorption was continuous beyond 28 days [9].

3.4. Phosphorous desorption kinetics

The desorption kinetics of P in the soil sample was investigated by making use of the DMT-HFAMO as the sorbent and it is mathematically represented by Equation (1).

$$SP \overset{K_R}{\rightarrow} Psol \overset{K_T}{\rightarrow} P_{HFAM}O \quad (1)$$

Where P_{sol} is P in the solution, SP is the solid phase P, k_T is the rate constant of P transport through the membrane, P_{HFAMO} is P adsorbed by HFAMO, and k_R is the rate constant of P released from soil.

The existence of two pools is presumed and pool A (SP_A) is the pool with the fast-release kinetics and pool B (SP_B) is the pool with the slow-release kinetics. By considering this assumption, the total exchangeable solid phase soil P (SP_{total}) at time t = 0 can be described using the mass balance equation presented in Equation (2).

$$SP_{total\ (0)} = SP_{A0} + SP_{B0} \quad (2)$$

Table 6
The comparison of phosphorus desorption between soil samples with the same treatments (n = 3).

Soil Samples	P Treatments (mg/kg)	Cumulative desorbed P (mg/kg) per Days				
		1	7	14	21	28
BD	0	z1.16 ± 0.01^{c}	y3.01 ± 0.09^{c}	x5.43 ± 0.18^{c}	w7.62 ± 0.09^{d}	v9.36 ± 0.16^{c}
KK	0	z1.01 ± 0.0^{d}	y3.27 ± 0.10^{b}	x5.75 ± 0.09^{b}	w7.99 ± 0.10^{c}	v9.57 ± 0.09^{b}
MS	0	z1.32 ± 0.02^{b}	y4.07 ± 0.09^{a}	x6.23 ± 0.10^{a}	w8.74 ± 0.09^{b}	v10.80 ± 0.16^{b}
NE	0	z1.43 ± 0.7^{a}	y4.02 ± 0.0^{a}	x6.39 ± 0.09^{a}	w9.01 ± 0.14^{a}	v11.29 ± 0.16^{a}
LSD (5%)		0.09	0.15	0.23	0.21	0.28
BD	50	z3.65 ± 0.11^{b}	y8.31 ± 0.14^{b}	x13.16 ± 0.03^{b}	w18.13 ± 0.24^{b}	v22.77 ± 0.34^{b}
KK	50	z4.30 ± 0.09^{a}	y9.74 ± 0.41^{a}	x14.99 ± 0.26^{a}	w20.06 ± 0.03^{a}	v24.36 ± 0.22^{a}
MS	50	z4.15 ± 0.09^{a}	y9.56 ± 0.11^{a}	x14.52 ± 0.32^{a}	w20.02 ± 0.44^{a}	v25.36 ± 0.55^{a}
NE	50	z4.12 ± 0.17^{a}	y9.78 ± 0.31^{a}	x14.89 ± 0.39^{a}	w20.14 ± 0.89^{a}	v24.55 ± 0.85^{a}
LSD (5%)		0.23	0.51	0.54	0.96	1.03
BD	100	z3.71 ± 0.06^{b}	y8.98 ± 0.44^{b}	x14.32 ± 0.79^{c}	w19.43 ± 0.92^{b}	v24.50 ± 0.78^{b}
KK	100	z4.57 ± 0.12^{a}	y10.12 ± 0.12^{a}	x15.84 ± 0.37^{b}	w21.18 ± 0.77^{a}	v25.84 ± 1.11^{b}
MS	100	z4.62 ± 0.22^{a}	y10.55 ± 0.36^{a}	x16.08 ± 0.36^{ab}	w21.67 ± 0.08^{a}	v27.45 ± 0.54^{a}
NE	100	z4.71 ± 0.14^{a}	y10.59 ± 0.14^{a}	x16.99 ± 0.53^{a}	w22.40 ± 0.67^{a}	v27.65 ± 0.46^{a}
LSD (5%)		0.28	0.56	1.03	1.30	1.45
BD	150	z4.70 ± 0.08b	y10.41 ± 0.9b	x16.09 ± 0.39c	w21.24 ± 0.31c	v26.86 ± 0.79^{c}
KK	150	z4.90 ± 0.17^{ab}	y10.73 ± 0.07b	x17.05 ± 0.48^{b}	w23.47 ± 0.49^{b}	v28.13 ± 0.55^{b}
MS	150	z5.19 ± 0.25^{a}	y11.93 ± 0.49^{a}	x18.35 ± 0.71^{a}	w24.06 ± 0.44^{ab}	v30.10 ± 0.27^{a}
NE	150	z5.23 ± 0.22^{a}	y11.91 ± 0.16^{a}	x18.52 ± 0.36^{a}	w24.32 ± 0.24^{a}	v30.35 ± 0.51^{a}
LSD (5%)		0.36	0.50	0.94	0.72	1.06

BD = Boji Dirmaji Soil, KK = Kiltu Kara Soil, MS = Mene Sibu Soil, n = Number of replications. Mean values in rows with different letters z, y, x, w and v are significantly different ($\alpha = 0.05$). Mean values in columns with different letters a, b, c and d are significantly different ($\alpha = 0.05$).

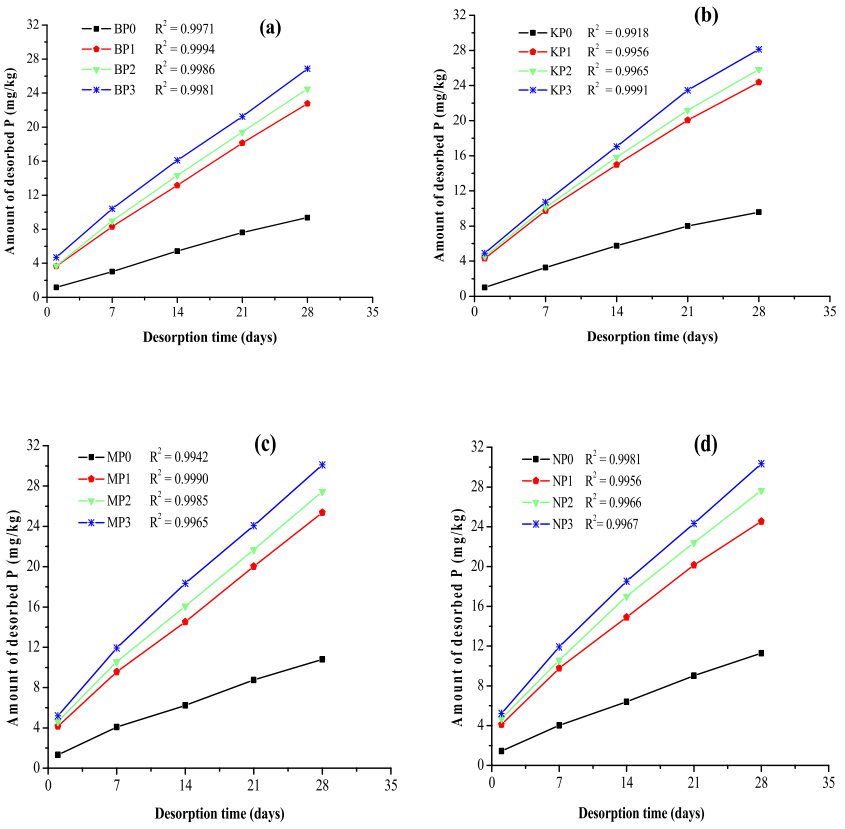

Fig. 4. Influence of added P on consecutive DMT-HFAMO extractable P over 28 days (a) Boji Dirmaji (b) Kiltu Kara (c) Mene Sibu (d) Nedjo Soil.

Where SP_{A0} and SP_{B0} are the initial amounts of P in pool A and pool B, respectively. The mass balance equation at time t is then given by Equation (3).

$$SP_{total\ (t)} = SP_{A(t)} + SP_{B(t)} \tag{3}$$

By taking the assumption that the decrease in SP_A and SP_B follow first-order kinetics, the integrated rate laws for the observed decrease can be given by Equation (4).

$$SP_{A(t)} = SP_{A0}e^{-kAt} \text{ and } SP_{B(t)} = SP_{B0}e^{-kBt} \tag{4}$$

Where k_A and k_B are the conditional first-order rate constants (day^{-1}) for P desorption from pool A and pool B, respectively. On the other hand, the total solid phase soil P ($SP_{total\ (t)}$) remaining at time t is given by Equation (5).

$$SP_{total\ (t)} = SP_{A0}\ e^{-kAt} + SP_{B0}\ e^{-kBt} \tag{5}$$

Similarly, the total quantity of P released at time t ($P_{R(t)}$) is described by Equation (6).

$$P_{R(t)} = SP_{A0} - SP_{A\ (t)} + SP_{B0} - SP_{B\ (t)}$$

$$= SP_{A0} - SP_{A0}\ e^{-kAt} + SP_{B0} - SP_{B0}\ e^{-kBt}, \text{ by rearranging this equation:}$$

$$= SP_{A0}\ (1- e^{-kAt}) + SP_{B0}\ (1- e^{-kBt}) \tag{6}$$

During the desorption process, it was taken into account that the rate constant of P release from the soil (K_R) was equal to the rate constant for P transport through the membrane (K_T) or the rate constant for the adsorption of P on the DMT-HFAMO, (k_A) which was obtained from the plot of the natural logarithm (ln) of the P desorbed by the DMT- HFAMO against time by taking the slope as k_A. Based on this, the phosphorus desorption kinetics of the soil samples were found to follow the first-order model which is described in equation (1), where k_d which was obtained to be in the range of 0.021–0.028 hr^{-1} is the rate constant of P desorption and it was comparable with literature reports [1,12] but greater than related similar reports [13,56].

As can be seen from Fig. 5, the rates of P-desorption from the soil samples which received different phosphorus treatments had no significant variation after 7 days of extraction time. This implies that the desorption proceeds in the same condition since the pore size of the membrane is similar to allow the passage of phosphate ions in a similar way except for the different P treatment. Desorption rates

of the first pool (SP_A) declined quickly in the first 14 days and become almost similar after 21 days which is in agreement with a similar study [54]. This indicates that the rate is fast and a reasonable amount of the applied P could be extracted over the first 14 days with DMT-HFAMO as the extraction is from the fast P-releasing pool. However, after the 14th day, the rate becomes low since the desorption could be from the fixed P and our finding agrees with the results of a similar study [14].

For the longer DMT-HFAMO extraction period (28th day), the desorption rate was less than 1.2 mg $kg^{-1}day^{-1}$ for all soil samples and it decreased for the different P applications (Fig. 5 a – d). The highest phosphate release was noted on the first extraction day with P3 (150 mg/kg) treatments for all soil samples. The results are in agreement with similar studies in the literature [57] that reported the kinetics of P release from soil can be described as an initial rapid rate followed by a slower rate. Thus, the kinetics study of soil is very important in that it can estimate the time frame by which the labile and fixed P could be available for plants in which other approaches can't pertain and the distribution of applied P fertilizer between labile and less labile forms can be determined. The SP_A/SP_B distribution ratio can also be used to assign soils under cultivation according to plant available P or potential P mobility [54].

3.5. Correlation of soil parameters with cumulative desorbed P

The relationship between the contents of physicochemical properties in the soil with cumulative desorbed phosphorus (CD28P) was analyzed by Pearson's correlation coefficient for each soil with different treatments (Table 7). The correlation coefficient values near +1 or −1 imply a good relationship between the two parameters and a correlation around zero implies no relationship between them at a significant level of 0.05 or 0.01 (Table 7).

A correlation value of $r > 0.7$ implies the parameters are strongly correlated, whereas r values between 0.5 and 0.7 indicate a moderate correlation between two different parameters [58]. When cumulative desorbed P correlated with contents of selected soil properties, low P-release was observed compared to total phosphorus, but higher as compared to available P (Table 4). It may be attributed due to the high content of Fe and Mn which fix P and low pH [13]. For example the negative significant relationship between soil pH (r = - 0.98) and similar manner for Mn_d (r = −1.00**) can reduce P desorption. This could be due to change of soluble phosphorus to insoluble magnesium and calcium phosphate results in reducing P availability in relation to the increase in soil pH [59, 60]. Bulk density of analyzed soil samples were inversely correlated (r = - 0.88) with cumulative desorbed P (CD28BP1) and is in agreement with related report [50].

Similarly, positive and highly significant correlations (r = 0.93), (r = 0.96) between cumulative desorbed P (CD28P) with P_T and P_{av}, respectively, for CD28BP0 and CD28NP0 were observed. In addition, negative significant correlation between CD28P and Mn_d (r = - 1.00*), between CD28P and Fe_{ox} (r = - 0.99) and between CD28P and Mn_{ox} (r = - 0.94) for KK soil indicate the strong correlation between these soil parameters and desorbed P (Table 7). This implies that as the P_{av}, pH and P_T increase in the soils, the amount of desorbed soil P increase. Moreover, as the extractable composition of Fe and Mn increases in the soils, the amount of desorbed soil P decreases. In short the physicochemical properties of the soil were strongly associated with cumulative desorbed P (CD28P).

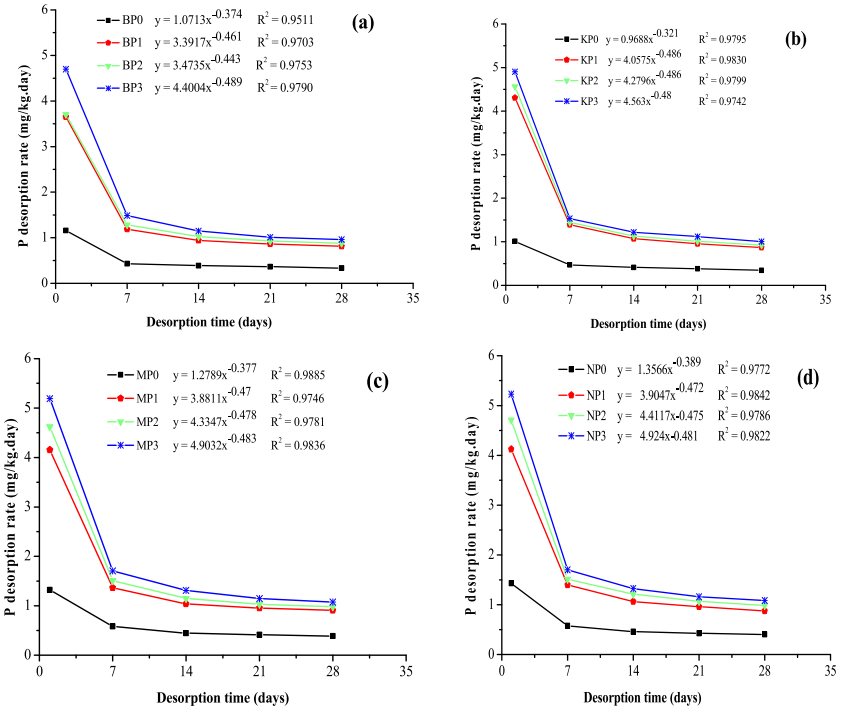

Fig. 5. Desorption rates for the different P treatments over 28 days (a) Boji Dirmaji (b) Kiltu Kara (c) Mene Sibu (d) Nedjo Soil.

Table 7
Correlation between soil properties and cumulative desorbed P with different treatments.

Soilsamples	Corre	pH_{H2O}	pH_{KCl}	EC	OC	OM	TN	CEC	B_d	P_{av}	EX.A	EX.Al	$EX.H^+$	Fe_{Ox}	Mn_{Ox}	Fe_d	Mn_d	P_T
BD	CD28BP0	−0.52	0.04	0.84	0.40	0.41	0.62	0.91	0.37	−0.15	−0.54	0.58	−0.72	−0.45	−0.89	−0.99	−0.96	0.93
	CD28BP1	−0.15	−0.67	−0.31	−0.89	−0.90	0.02	−0.97	−0.88	−0.52	0.95	0.08	0.11	−0.23	0.98	0.85	0.92	−0.48
	CD28BP2	−0.90	−0.99	0.61	−0.88	−0.87	0.83	−0.34	−0.90	−0.99[a]	0.79	0.86	−0.76	−0.93	0.38	0.06	0.20	0.50
	CD28BP3	0.42	−0.15	−0.78	−0.50	−0.51	−0.53	−0.95	−0.47	0.04	0.62	−0.48	0.64	0.35	0.93	0.99[a]	0.98	−0.88
KK	CD28KP0	−0.45	−0.77	−0.77	−0.61	−0.60	−0.23	−0.98	0.17	−0.99	−0.93	−0.64	−0.93	−0.34	−0.94	0.07	−0.77	−0.22
	CD28KP1	−0.91	−1.00**	−1.00**	−0.97	−0.97	−0.79	−0.64	−0.49	−0.87	−0.95	−0.01	−0.95	−0.86	−0.51	0.68	−1.00**	0.45
	CD28KP2	0.79	0.97	0.97	0.90	0.89	0.64	0.80	0.28	0.96	1.00	0.24	1.00	0.72	0.69	−0.50	0.97	−0.23
	CD28KP3	−0.98	−0.82	−0.82	−0.92	−0.93	−1.00[a]	−0.07	−0.91	−0.42	−0.59	0.57	−0.59	−0.99	0.09	0.98	−0.82	0.89
MS	CD28MP0	−0.99	0.87	−0.39	−0.89	−0.87	−0.97	−0.51	−1.00	−0.29	0.99	−0.51	0.96	0.64	−0.07	0.98	−0.61	−0.68
	CD28 MP1	0.96	−0.94	0.53	0.80	0.79	0.91	0.64	0.99[a]	0.13	−1.00[a]	0.64	−0.99	−0.51	−0.09	−0.93	0.73	0.56
	CD28 MP2	−0.24	0.77	−1.00[a]	0.11	0.13	−0.12	−0.99	−0.46	0.79	0.49	−0.99	0.60	−0.48	0.90	0.17	−0.96	0.43
	CD28 MP3	−0.38	−0.25	0.80	−0.67	−0.69	−0.49	0.70	−0.15	−0.99[a]	0.11	0.70	−0.01	0.90	−0.98	0.44	0.62	−0.88
NE	CD28NP0	0.23	0.97	−0.29	−0.65	−0.66	0.96	−1.00**	−0.29	0.91	−0.23	−0.84	−0.04	−0.96	0.68	0.01	0.53	0.67
	CD28 NP1	−0.74	0.67	−0.98	−0.98	−0.98	0.21	−0.47	−0.98	0.80	0.74	0.07	0.85	−0.21	0.97	−0.87	0.99[a]	0.34
	CD28 NP2	−0.99	0.14	−0.93	−0.69	−0.68	−0.38	0.11	−0.93	0.32	0.99	0.62	0.99[a]	0.38	0.66	−1.00	0.79	−0.81
	CD28 NP3	−0.69	0.73	−0.96	−0.99	−0.99	0.29	−0.54	−0.96	0.85	0.69	−0.01	0.81	−0.29	0.99	−0.83	1.00[a]	0.27

[a] *Correlation is significant at the 0.05 level (2-tailed)* and ** = *Correlation is significant at the 0.01 level (2-tailed), Corre = Correlation and CD28P = Cumulative desorbed P for each treatments (P0* (0 mg/kg)*, P1* (50 mg/kg)*, P2* (100 mg/kg) *and P3* (150 mg/kg)*).*

4. Conclusion

The knowledge regarding the soil P fixing capacity of soil is very important for effective fertilizer application. In view of this, magnetic $Fe_3O_4/Al_2O_3/MnO_2$ mixed oxide ternary nanocomposite was successfully synthesized by co-precipitation method and used for phosphate desorption study. The as-synthesized nanocomposite was characterized by different analytical methods and the one with a crystalline size of 22.75 nm and surface area of 203.69 ± 1.34 m^2/g was selected and used to conduct the desorption study by filing it in dialysis membrane tubes. As observed from the results, the selected ternary nanocomposite was found to exhibit high sorption capacity and faster desorption rate as compared to a single system as well as other ternary mixed oxide nanocomposites in which we have previously synthesized for the same purpose on similar soil. The highest cumulative desorption was obtained from P3 treatment for all soil samples BD (4.70–26.86), KK (4.90–28.13), MS (5.19–30.10) and NE(5.23–30.35 mg/kg) over 1–28 days treatment time and lower at P0 treatment for all soil samples. Therefore, the $Fe_3O_4/Al_2O_3/MnO_2$ mixed oxide ternary nanocomposite-filled dialysis membrane tube can be taken as a promising analytical method for measuring fixed-P availability by simulating it as a plant does with high P-desorption efficiency and rapid P-release capacity from acidic soil which is vital advantage for fertilizer recommendation for agricultural activity.

Data availability

Not applicable.

Funding

Grants of HURG-2016-03-02 and HURG-2020–03–02–75 were provided by Haramaya University (Ethiopia).

CRediT authorship contribution statement

Hirpo Hinsene: Writing – original draft, Investigation, Formal analysis. **Abi M.Taddesse:** Writing – review & editing, Supervision, Funding acquisition, Conceptualization. **Endale Teju:** Writing – review & editing, Supervision, Methodology, Data curation. **Yibrehu Bogale:** Writing – review & editing, Software, Resources.

Declaration of competing interest

The authors declare that they have no known competing financial interests or personal relationships that could have appeared to influence the work reported in this paper.

Acknowledgments

The authors are very much grateful for the support of the Department of Chemistry, College of Natural and Computational Sciences, Haramaya University, Ethiopia.

References

[1] M. Kamper, A.S. Claassens, Exploitation of soil by Roots as influenced by phosphorus applications, Commun. Soil Sci. Plant Anal. 36 (1–3) (2005) 393–402, https://doi.org/10.1081/CSS-200043109.
[2] R.W. McDowell, I. Stewart, The phosphorus composition of contrasting soils in pastoral, native and forest management in Otago, New Zealand: sequential extraction and 31P NMR, Geoderma 130 (1) (2006) 176–189, https://doi.org/10.1016/j.geoderma.2005.01.020.
[3] J.J. Weeks Jr., G.M. Hettiarachchi, A review of the latest in phosphorus fertilizer technology: possibilities and pragmatism, J. Environ. Qual. 48 (5) (2019) 1300–1313, https://doi.org/10.2134/jeq2019.02.0067.
[4] Z. Xiaoyang, X. Minggang, W. Boren, C. Zejiang, C. Gilles, Changes of soil phosphorus fractionation according to pH in red soils of China: an incubation experiment, Commun. Soil Sci. Plant Anal. 49 (7) (2018) 791–802, https://doi.org/10.1080/00103624.2018.1435676.
[5] R. Indiati, Addition of phosphorus to soils with low to medium phosphorus retention capacities. II. effect on soil phosphorus extractability, Commun. Soil Sci. Plant Anal. 31 (15–16) (2000) 2591–2606, https://doi.org/10.1080/00103620009370610.
[6] M. Abrams, W.M. Jarrell, Bioavailability index for phosphorus using ion exchange resin impregnated membranes, Soil Sci. Soc. Am. J. 56 (5) (1992) 1532–1537, https://doi.org/10.2136/sssaj1992.03615995005600050033x.
[7] G.F. Koopmans, M.E. van der Zeeuw, W.J. Chardon, J. Dolfing, Selective extraction of labile phosphorus using dialysis membrane tubes filled with hydrous iron hydroxide, Soil Sci. 166 (7) (2001).
[8] R. Lookman, D. Freese, R. Merckx, K. Vlassak, W.H. van Riemsdijk, Long-term kinetics of phosphate release from soil, Environ. Sci. Technol. 29 (6) (1995) 1569–1575, https://doi.org/10.1021/es00006a020.
[9] A.M. Taddesse, A.S. Claassens, P.C. de Jager, Long-term phosphorus desorption using dialysis membrane tubes filled with iron hydroxide and its effect on phosphorus pools, J. Plant Nutr. 31 (8) (2008) 1507–1522, https://doi.org/10.1080/01904160802208683.
[10] A.M. Taddesse, A.S. Claassens, P.C. de Jager, Long-term kinetics of phosphate desorption from soil and its relationship with plant growth, S. Afr. J. Plant Soil 25 (3) (2008) 131–134, https://doi.org/10.1080/02571862.2008.10639907.
[11] Y.B. Dibabe, A.M. Taddesse, E. Teju, Y. Bogale, Hydrous Fe-Al-Zr oxide composite filled dialysis membrane tubes for phosphate desorption study from acidic soils, Environ. Nanotechnol. Monit. Manag. 18 (2022) 100723, https://doi.org/10.1016/j.enmm.2022.100723.
[12] D. Freese, R. Lookman, R. Merckx, W. Van Riemsdijk, New method for assessment of long-term phosphate desorption from soils, Soil Sci. Soc. Am. J. 59 (5) (1995) 1295–1300, https://doi.org/10.2136/sssaj1995.03615995005900050013x.
[13] G. Shumi, A. Tadasse, T. Kebede, Phosphorus desorption study using dialysis membrane tube filling fe-al-mn ternary mixed nanocomposite from different f arming practice of acidic soil, Chem. Mater. Res. 7 (8) (2015) 82–91.

[14] V. Ochwoh, E. Nankya, P. De Jager, A. Claassens, The impact of phosphorous applications and incubation periods on p-desorption characteristics with successive DMT-HFO-P extractions on P fixing soils, Int. J. Phys. Soc. Sci. 13 (6) (2016) 1–14.

[15] A. Chimdi, H. Gebrekidan, K. Kibret, A. Tadesse, Response of barley to liming of acid soils collected from different land use systems of Western Oromia, Ethiopia, J. Biodivers. Environ. Sci. (JBES) 2 (7) (2012) 1–13.

[16] A. Deressa, Evaluation of soil acidity in agricultural soils of smallholder farmers in South Western Ethiopia, Sci. Technol. Arts Res. J. 2 (2) (2013) 1–6, https://doi.org/10.4314/star.v2i2.98859.

[17] L. Poggio, B. Vrščaj, R. Schulin, E. Hepperle, F.A. Marsan, Metals pollution and human bioaccessibility of topsoils in Grugliasco (Italy), Environ. Pollut. 157 (2) (2009) 680–689, https://doi.org/10.1016/j.envpol.2008.08.009.

[18] L. Chai, Y. Wang, N. Zhao, W. Yang, X. You, Sulfate-doped Fe_3O_4/Al_2O_3 nanoparticles as a novel adsorbent for fluoride removal from drinking water, Water Res. 47 (12) (2013) 4040–4049, https://doi.org/10.1016/j.watres.2013.02.057.

[19] A. Durdureanu-Angheluta, M. Pinteala, B. Simionescu, Tailored and functionalized magnetite particles for biomedical and industrial applications, Mater. Sci. Technol. (2012) 149–178, https://doi.org/10.5772/30217.

[20] S. Laurent, D. Forge, M. Port, A. Roch, C. Robic, L. Vander Elst, et al., Magnetic iron oxide nanoparticles: synthesis, stabilization, vectorization, physicochemical characterizations, and biological applications, Chem. Rev. 108 (6) (2008) 2064–2110, https://doi.org/10.1021/cr068445e.

[21] J.-S. Jiang, Z.-F. Gan, Y. Yang, B. Du, M. Qian, P. Zhang, A novel magnetic fluid based on starch-coated magnetite nanoparticles functionalized with homing peptide, J. Nanoparticle Res. 11 (6) (2009) 1321–1330, https://doi.org/10.1007/s11051-008-9534-5.

[22] F. Tsegaye, A.M. Taddesse, E. Teju, M. Aschalew, Preparation and sorption property study of $Fe_3O_4/Al_2O_3/ZrO_2$ composite for the removal of cadmium, lead and chromium ions from aqueous solutions, Bull. Chem. Soc. Ethiop. 34 (1) (2020) 105–121, https://doi.org/10.4314/bcse.v34i1.10.

[23] A. Chimdi, Assessment of the severity of acid saturations on soils collected from cultivated lands of East Wollega Zone, Ethiopia, Sci. Technol. Arts Res. J. 3 (4) (2015) 42–48, https://doi.org/10.4314/star.v3i4.6.

[24] G.J. Bouyoucos, Hydrometer method improved for making particle size analyses of soils, Agron. J. 54 (5) (1962) 464–465, https://doi.org/10.2134/agronj1962.00021962005400050028x.

[25] J.M. Moreno-Maroto, J. Alonso-Azcarate, Evaluation of the USDA soil texture triangle through Atterberg limits and an alternative classification system, Appl. Clay Sci. 229 (2022) 106689, https://doi.org/10.1016/j.clay.2022.106689.

[26] J.J. Drewry, B.A. Stevenson, S.J. McNeill, J.-A.E. Cavanagh, M.D. Taylor, Impact of volumetric versus gravimetric assessment on Olsen P concentrations, N. Z. J. Agric. Res. 65 (6) (2022) 463–483, https://doi.org/10.1080/00288233.2021.1912118.

[27] A. Walkley, I.A. Black, An examination of the Degtjareff method for determining soil organic matter, and a proposed modification of the chromic acid titration method, Soil Sci. 37 (1) (1934) 29–38.

[28] C. Achalu, G. Heluf, K. Kibebew, Phosphorus desorption patterns of soils from different land use systems of East Wollega, Ethiopia, Middle East J. Sci. Res. 17 (2) (2013) 245–251, https://doi.org/10.5829/idosi.mejsr.2013.17.02.12197.

[29] R.H. Bray, L.T. Kurtz, Determination of total, organic, and available forms of phosphorus in soils, Soil Sci. 59 (1) (1945) 39–46.

[30] O.P. Mehra, M.L. Jackson, IIron oxide removal from soils and clays by a dithionite-citrate system buffered with sodium bicarbonate, Clay Clay Miner. (2013) 317–327, https://doi.org/10.1016/B978-0-08-009235-5.50026-7.

[31] F. Kassahun, A.M. Taddesse, E. Teju, Y. Bogale, Magnetic $Al_2O_3/ZrO_2/Fe_3O_4$ nanocomposite: synthesis, characterization, and application for the adsorptive removal of nitrate from aqueous solution, Groundwater for Sustainable Development 20 (2023) 100873, https://doi.org/10.1016/j.gsd.2022.100873.

[32] B. Abebe, A.M. Taddesse, T. Kebede, E. Teju, I. Diaz, Fe-Al-Mn ternary oxide nanosorbent: synthesis, characterization and phosphate sorption property, J. Environ. Chem. Eng. 5 (2) (2017) 1330–1340, https://doi.org/10.1016/j.jece.2017.02.026.

[33] F. Gulshan, Y. Kameshima, A. Nakajima, K. Okada, Preparation of alumina–iron oxide compounds by gel evaporation method and its simultaneous uptake properties for Ni^{2+}, NH_4^+ and $H_2PO_4^-$, J. Hazard Mater. 169 (1) (2009) 697–702, https://doi.org/10.1016/j.jhazmat.2009.04.009.

[34] A.S. Tofik, A.M. Taddesse, K.T. Tesfahun, G.G. Girma, Fe–Al binary oxide nanosorbent: synthesis, characterization and phosphate sorption property, J. Environ. Chem. Eng. 4 (2) (2016) 2458–2468, https://doi.org/10.1016/j.jece.2016.04.023.

[35] A.M. Dinkirie, A.M. Tadesse, T.J. Kebede, Chelating agent-free solid phase extraction (CAF-SPE) of uranium, cadmium and lead by Fe-Al-Mn nanocomposite from aqueous solution 33 (26) (2022) 21034–21047, https://doi.org/10.1007/s10854-022-08908-0.

[36] X. Liu, N. Wu, C. Cui, N. Bi, Y. Sun, One pot synthesis of Fe_3O_4/MnO_2 core–shell structured nanocomposites and their application as microwave absorbers, RSC Adv. 5 (31) (2015) 24016–24022, https://doi.org/10.1039/C4RA14753G.

[37] T. Herranz, S. Rojas, M. Ojeda, F.J. Pérez-Alonso, P. Terreros, K. Pirota, et al., Synthesis, structural features, and reactivity of Fe−Mn mixed oxides prepared by microemulsion, Chem. Mater. 18 (9) (2006) 2364–2375, https://doi.org/10.1021/cm052568i.

[38] M.A. Raza, Z. Kanwal, A. Rauf, A.N. Sabri, S. Riaz, S. Naseem, Size- and shape-dependent antibacterial studies of silver nanoparticles synthesized by wet chemical routes, Nanomaterials 6 (4) (2016) 74–79, https://doi.org/10.3390/nano6040074.

[39] S. Cava, S.M. Tebcherani, I.A. Souza, S.A. Pianaro, C.A. Paskocimas, E. Longo, et al., Structural characterization of phase transition of Al_2O_3 nanopowders obtained by polymeric precursor method, Mater. Chem. Phys. 103 (2) (2007) 394–399, https://doi.org/10.1016/j.matchemphys.2007.02.046.

[40] C.-Y. Cao, J. Qu, W.-S. Yan, J.-F. Zhu, Z.-Y. Wu, W.-G. Song, Low-cost synthesis of flowerlike α-Fe_2O_3 nanostructures for heavy metal ion removal: adsorption property and mechanism, Langmuir 28 (9) (2012) 4573–4579, https://doi.org/10.1021/la300097y.

[41] Y. Wang, X. Zhao, J. Yan, An application of nano-technology in environmental protection, Shanghai Environmental Science 23 (4) (2004) 178–181.

[42] M.G. Sujana, S. Anand, Iron and aluminium based mixed hydroxides: a novel sorbent for fluoride removal from aqueous solutions, Appl. Surf. Sci. 256 (23) (2010) 6956–6962, https://doi.org/10.1016/j.apsusc.2010.05.006.

[43] J. Lǚ, H. Liu, R. Liu, X. Zhao, L. Sun, J. Qu, Adsorptive removal of phosphate by a nanostructured Fe–Al–Mn trimetal oxide adsorbent, Powder Technol. 233 (2013) 146–154, https://doi.org/10.1016/j.powtec.2012.08.024.

[44] N.R. Habib, A.M. Taddesse, A. Temesgen, Synthesis, characterization and photocatalytic activity of $Mn_2O_3/Al_2O_3/Fe_2O_3$ nanocomposite for degradation of malachite green, Bull. Chem. Soc. Ethiop. 32 (1) (2018) 101–109.

[45] G. Zhang, H. Liu, R. Liu, J. Qu, Removal of phosphate from water by a Fe–Mn binary oxide adsorbent, J. Colloid Interface Sci. 335 (2) (2009) 168–174, https://doi.org/10.1016/j.jcis.2009.03.019.

[46] T.O. Fufa, Abi Tadesse Mengesha, Om Prakash Yadav, Synthesis, characterization and photocatalytic activity of $MnO_2/Al_2O_3/Fe_2O_3$ nanocomposite for phenol degradation, Chem. Mater. Res. 6 (2014) 73–86.

[47] I. Nedkov, T. Merodiiska, L. Slavov, R.E. Vandenberghe, Y. Kusano, J. Takada, Surface oxidation, size and shape of nano-sized magnetite obtained by co-precipitation, J. Magn. Magn Mater. 300 (2) (2006) 358–367, https://doi.org/10.1016/j.jmmm.2005.05.020.

[48] A. Kidanemariam, H. Gebrekidan, T. Mamo, K. Kibret, Impact of altitude and land use type on some physical and chemical properties of acidic soils in Tsegede Highlands, Northern Ethiopia, Open J. Soil Sci. 2 (3) (2012) 223.

[49] M. Aytenew, Effect of slope gradient on selected soil physicochemical properties of dawja watershed in Enebse sar Midir district, Amhara National regional state, Am. J. Sci. Ind. Res. 6 (4) (2015) 74–81.

[50] A. Worku, B. Bedadi, Studies on soil physical properties of salt affected soil in Amibara area, central rift valley of Ethiopia, International Journal of Agricultural Sciences Natural Resources 3 (2) (2016) 8–17.

[51] D. Solomon, J. Lehmann, T. Mamo, F. Fritzsche, W. Zech, Phosphorus forms and dynamics as influenced by land use changes in the sub-humid Ethiopian highlands, Geoderma 105 (1) (2002) 21–48, https://doi.org/10.1016/S0016-7061(01)00090-8.

[52] P.A. Sanchez, C.A. Palm, S.W. Buol, Fertility capability soil classification: a tool to help assess soil quality in the tropics, Geoderma 114 (3) (2003) 157–185, https://doi.org/10.1016/S0016-7061(03)00040-5.

[53] O.O. Olatunji, Y. Oyeyiola, G.O. Oyediran, Assessment of dithionite and oxalate extractable iron and aluminium oxides on a landscape on basement complex soil in South-Western Nigeria, Open J. Soil Sci. 5 (11) (2015) 266–275, https://doi.org/10.4236/ojss.2015.511025.

[54] A. Reyhanitabar, S. Heidari, S. Oustan, R. Gilkes, A modified DMT-HFO technique for investigating the kinetics of phosphorus desorption from calcareous soils and its relationship with maize growth, Commun. Soil Sci. Plant Anal. 49 (11) (2018) 1281–1288, https://doi.org/10.1080/00103624.2018.1457156.
[55] V.A. Ochwoh, A.S. Claassens, P.C. de Jager, Chemical changes of applied and native phosphorus during incubation and distribution into different soil phosphorus pools, Commun. Soil Sci. Plant Anal. 36 (4–6) (2005) 535–556, https://doi.org/10.1081/CSS-200043281.
[56] A.M. Taddesse Asc, P.C. De Jager, Long term kinetics of phosphate desorption from soil and its relationship with plant growth, S. Afr. J. Plant Soil 25 (2008) 131–134.
[57] M. Jalali, N. Ahmadi Mohammad Zinli, Kinetics of phosphorus release from calcareous soils under different land use in Iran, J. Plant Nutr. Soil Sci. 174 (1) (2011) 38–46.
[58] M.R. Sharma, N. Raju, Correlation of heavy metal contamination with soil properties of industrial areas of Mysore, Karnataka, India by cluster analysis, Int. Res. J. Environ. Sci. 2 (10) (2013) 22–27.
[59] Z. Bhat, S. Padder, A. Ganaie, N. Dar, H. Rehman, M. Wani, Correlation of available nutrients with physico-chemical properties and nutrient content of grape orchards of Kashmir, J. Pharmacogn. Phytochem. 6 (2) (2017) 181–185.
[60] R. Patil, R. Saler, V. Gaikwad, Nutritional survey of different vineyards in Nashik district, Mahararashtra Journal of Basic Sciences 1 (2015) 6–12.